OPEN ACCESS
IOP Publishing
Journal of Physics: Condensed Matter
J. Phys.: Condens. Matter **32** (2020) 255802 (10pp)
https://doi.org/10.1088/1361-648X/ab7ad6

Torque magnetometry study of the spin reorientation transition and temperature-dependent magnetocrystalline anisotropy in $NdCo_5$

Santosh Kumar, Christopher E Patrick, Rachel S Edwards, Geetha Balakrishnan, Martin R Lees and Julie B Staunton

Department of Physics, University of Warwick, Coventry CV4 7AL, United Kingdom

E-mail: santosh.kumar595@gmail.com

Received 15 October 2019, revised 30 January 2020
Accepted for publication 27 February 2020
Published 25 March 2020

Abstract

We present the results of torque magnetometry and magnetic susceptibility measurements to study in detail the spin reorientation transition (SRT) and magnetic anisotropy in the permanent magnet $NdCo_5$. We further show simulations of the measurements using first-principles calculations based on density-functional theory and the disordered local moment picture of magnetism at finite temperatures. The good agreement between theory and experimental data leads to a detailed description of the physics underpinning the SRT. In particular we are able to resolve the magnetization of, and to reveal a canting between, the Nd and Co sublattices. The torque measurements carried out in the *ac* and *ab* planes near the easy direction allow us to estimate the anisotropy constants, K_1, K_2 and K_4 and their temperature dependences. Torque curves, $\tau(\gamma)$ recorded by varying the direction of a constant magnetic field in the crystallographic *ac* plane show a reversal in the polarity as the temperature is changed across the SRT ($240 < T < 285$ K). Within this domain, $\tau(\gamma)$ exhibits unusual features different to those observed above and below the transition. The single crystals of $NdCo_5$ were grown using the optical floating zone technique.

Keywords: torque magnetometry, spin reorientation transition, magnetocrystalline anisotropy

Supplementary material for this article is available online

(Some figures may appear in colour only in the online journal)

1. Introduction

Permanent magnets based on the rare-earth transition-metal series, RCo_5 (R = rare earth) [1, 2] display useful magnetic properties over a wide temperature range, making these materials suitable candidates for a number of applications. These properties include high magnetic ordering temperatures, large saturation magnetization (M_s), and significant magnetocrystalline anisotropy (MCA). The latter characterizes variations in the magnetic response of the material when a magnetic field is applied along different crystallographic axes. The magnetic anisotropy can also play a role in governing important properties such as the coercivity of a magnet. As a result, studies focussing on the MCA in RCo_5 have been an important area of research for several decades [3–21].

RCo_5 crystallizes in a hexagonal structure (space group of $P6/mmm$) [22]. The spin moments of the Co atoms align antiferromagnetically with the R spin moment. However, the total

R moment can align ferromagnetically or antiferromagnetically with the Co moments, depending on the magnitude and direction of the orbital contribution. RCo_5 is therefore best described as a ferrimagnet, and its magnetic properties derive from the individual R and Co sublattices.

The Co sublattice provides a large contribution to the magnetization and is also responsible for the high ordering temperature. There is also a significant contribution to the MCA from the Co moments, which can be clearly seen in compounds with nonmagnetic Rs like YCo_5 [6] and $LaCo_5$ [23]. However, it is the R atoms which can dramatically affect the MCA, thanks to their unfilled 4f shells interacting with the crystal field.

The ordering of the R moments is driven by the Co sublattice through an exchange field, which although being of order 200 T is relatively weak compared to the exchange between the Co moments themselves. Accordingly, as the temperature increases, the R moments disorder at a faster rate than the Co. The balance between R and Co contributions to the magnetic properties therefore shifts, with Co becoming progressively more important as the temperature increases.

One of the clearest examples of this shifting balance is in the spin reorientation transitions of $NdCo_5$ [12, 17, 24–28]. The Nd^{3+} ion, thanks to its negative Stevens coefficient, prefers to have its magnetization pointing in the basal plane of the RCo_5 structure [29]. The Co atoms, however, prefer to have their moments pointing along the c axis, (e.g. YCo_5 and $LaCo_5$). At lower temperatures ($T < 240$ K), the Nd contribution dominates the MCA, and the easy axis of magnetization lies in the basal (ab) plane. However this contribution diminishes as the Nd moments become more disordered with temperature, and above 280 K Co dominates so that the material favours an easy c axis. In the intermediate region $240 < T < 280$ K there is spin reorientation transition (SRT) from easy-plane to easy-axis configurations.

Usually, SRTs are analysed in terms of the anisotropy constants K_i, which for a hexagonal system are related to the free energy density E through:

$$E = K_1 \sin^2\theta + K_2 \sin^4\theta + K_3 \sin^6\theta + K_4 \sin^6\theta \cos 6\phi, \quad (1)$$

where θ and ϕ are the polar and azimuthal angles respectively of the magnetization. It is important to note that the magnetization contained in equation (1) is the vector sum of the individual contributions from the Nd and Co sublattices. Although the exchange interaction will tend to favour collinear alignment of these sublattices, the application of an external field (e.g. in an experimental measurement) might induce a canting as the system tries to minimize its overall energy (Zeeman, exchange and anisotropy). Only in the limit of strong exchange or weak external field will the sublattices remain collinear, with the anisotropy constants K_i then reducing to a simple sum of the individual MCA contributions from Nd and Co. Generally, K_i are instead effective values, which include the interactions with the exchange and external fields. In $GdCo_5$ these interactions are responsible for a softening of K_1 by 50 percent compared to YCo_5 [21].

Despite their complicated microscopic origin, K_i remain convenient tools to characterize the anisotropic properties of ferromagnets and ferrimagnets alike. $NdCo_5$ has been the subject of a large number of studies aimed at measuring K_i and their dependence on temperature [8, 12, 17, 28]. Unfortunately, there is considerable variation in the values reported in the literature. This may be due, in part, to the fact that the samples studied were of different forms, including thin films [28], aligned powders [12] and single crystals [8, 17]; the best estimates of K_i are usually expected from measurements performed on high-quality single crystals.

Another potential source of variation in K_i is the experimental measurement technique and subsequent analysis. The most common technique exploited to study MCA is dc magnetometry within the Sucksmith–Thompson method [30]. This method requires making two sets of magnetization measurements, along the easy and hard axes, which are then combined and fitted to a model to yield K_i. A more direct link to MCA-related properties should be provided by torque magnetometry, which probes the derivative of equation (1) with respect to field angle. This technique was developed a number of years ago, and measurement equipment has become a standard feature of commercially available Physical Property Measurement System (PPMS) units. However, there is a shortage of examples in the literature which clearly demonstrate how one goes from raw data to K_i values, especially in R–TM magnets where K_i is large.

With these factors in mind, and given the status of $NdCo_5$ as a prototypical R–Co magnet exhibiting SRT phenomena (also attracting interest for potential magnetocaloric applications [27]) we have performed a detailed study of this material. In particular, we have focussed on developing new routes to grow high quality single crystals of $NdCo_5$, used anisotropy measurements to establish the temperature dependence of the K_i's, and completed a microscopic interpretation of the K_i values by *ab initio* calculations [31] to determine the nature of the SRT in $NdCo_5$.

Single crystals of $NdCo_5$ were synthesized using the optical floating zone technique (FZT) [32], a method normally used to grow oxide and refractory materials, and not previously applied to $NdCo_5$. The crystal growth of the RCo_5 family of compounds has always been challenging owing to their higher melting points, formation via a peritectic reaction, and the reaction of the material in the molten state with the container (crucible) utilized during the growth [33]. Overcoming these difficulties, we have successfully employed the FZT (crucible free growth) to grow $NdCo_5$ single crystals.

To measure the anisotropy constants we performed torque magnetometry, taking particular care to show how the structure of the torque curves when the field is applied close to the easy direction can be used to extract K_i. Finally, we performed first-principles calculations based on density-functional theory to construct theoretical torque curves that can be compared directly to the experimental data. These calculations use a recently-developed method [31] which takes into account the finite temperature disorder of the magnetic moments including the interaction of the rare earth moment with the crystal field. The calculations allow the total magnetization to be resolved into R and Co components, elucidating the underlying physics of the SRT. Furthermore, since the calculations describe a

single magnetic particle, comparison between the theory and experiment allow the effects of magnetic domains to be evaluated. Intuitively, the agreement between theory and experiment is best when the external field is applied close to the easy direction (where the domain structure is removed by the field), validating the scheme used to extract K_i. Our study clearly demonstrates the utility of torque magnetometry as an important tool for studying the magnetic anisotropy in this class of materials. We have also established a new route, namely the FZT, to synthesize single crystals of the RCo_5 compounds.

The rest of our manuscript is ordered as follows. In section 2 we describe the experimental techniques used to synthesize the $NdCo_5$ crystals and characterize their magnetic properties. We also describe the scheme used to extract anisotropy constants from the torque measurements, and give an overview of the first-principles method of calculating torque curves. In section 3 we show our results, and give conclusions in section 4.

2. Methods

2.1. Experimental techniques

Polycrystalline buttons of $NdCo_5$ were synthesized by arc melting high purity Nd and Co elements in stoichiometric proportions on a water-cooled copper hearth in an argon atmosphere. The buttons were then cast in the shape of a cylindrical rod ($\approx$ 30 mm in length) for use as the feed rod for the single crystal growth by the FZT [32] using a four mirror xenon arc lamp optical image furnace (CSI FZ-T-12000-X-VI-VP, Crystal Systems Inc., Japan). A tungsten rod was used as the seed for the growth. The growth chamber was evacuated and backfilled with high purity Ar gas to a pressure of 4.5 bar for the growth. The crystal growth was carried out at a speed of 20 mm h^{-1} with the feed and seed rods rotating in opposite directions. Single crystal pieces suitable for the studies were isolated from the as-grown boule. The quality of the $NdCo_5$ single crystals was examined through x-ray Laue backscattering. One crystal taken from the boule, adjacent to the piece used for the magnetization measurements, was further characterized by single crystal x-ray diffraction (Gemini R equipped with dual wavelength (Cu/Mo) fine x-ray sources) at room temperature. The data confirm that $NdCo_5$ crystallizes in the $P6/mmm$ space group, with lattice parameters $a = b = 5.008(4)$ Å and $c = 3.991(6)$ Å in agreement with reported values [22].

To carry out the dc magnetization, ac susceptibility, and torque magnetometry measurements, an irregular-shaped single crystal with a mass of 0.053 mg was selected. The reasons for using such a small sample are discussed below. Exploiting the anisotropy of the system, the single-crystal was aligned in slow setting epoxy in a mould at 298 K in the presence of a magnetic field ($\mu_0 H \approx 0.2$ T). At this temperature, the c axis is the easy axis of magnetization.

Magnetization measurements as a function of temperature or applied field were carried out in a Quantum Design (QD) Magnetic Property Measurement System (MPMS) superconducting quantum interference device (SQUID) magnetometer. AC susceptibility measurements as a function of temperature were also performed in the MPMS. The amplitude of the ac field was $h_{ac} = 0.3$ mT with a frequency of 10 Hz.

Torque magnetometry measurements were performed in a QD PPMS. A torque lever chip with a Wheatstone bridge circuit measures the change in resistance of piezoresistor grids on the legs of the lever due to a magnetic torque. The chip was mounted (without a sample) on a rotator and calibrated in the temperature range 1.8 to 320 K in fields as high as 9 T. To carry out the torque measurements, the sample was attached at the centre of the chip using Apiezon™ N grease or cyanolite glue. We studied the angular variation of torque, τ, while the direction of the applied magnetic field is varied in either the *ac* plane or within the *ab* plane of $NdCo_5$.

We found that the values of the anisotropy constants K_1, K_2 and K_4 and M_s estimated in the present study using torque magnetometry are dependent on the size of the sample. Using YCo_5, a simpler system with a single magnetic sublattice and which does not show any SRT, we found that in order to determine the anisotropy constants accurately using the QD PPMS system, the sample volume has to be below a certain threshold.

2.2. Theoretical background

Using equation (1) for the free energy, the easy direction is found by minimizing E with respect to the magnetization angles. The azimuthal angle ϕ is 0 or 30° for negative and positive K_4, respectively. The values of the polar angle θ corresponding to maxima or minima of E satisfy

$$\sin 2\theta \left[K_1 + 2K_2 \sin^2\theta + 3K_3' \sin^4\theta\right] = 0, \qquad (2)$$

where $K_3' = K_3 - |K_4|$. The $\sin 2\theta$ term corresponds to $\theta = 0$ (axis) or $\theta = 90°$ (plane) solutions, whilst the term in the square brackets corresponds to the canted (cone) solution.

For analysis of the spin reorientation transition in $NdCo_5$, we note that based on magnetization measurements Ohkoshi *et al* [17] concluded that the effect of K_3' was negligible. Therefore, we drop the K_3' term in equation (2), which gives the following expression for the easy angle α for cone anisotropy:

$$\alpha = \sin^{-1}\left(\sqrt{-\frac{K_1}{2K_2}}\right). \qquad (3)$$

From the second derivatives of E we obtain the condition for cone anisotropy to be ($K_1 < 0$; $K_1 + 2K_2 > 0$). Easy axis anisotropy requires ($K_1 > 0$; $K_1 + K_2 > 0$), and otherwise the anisotropy is easy plane ($K_1 < 0$; $K_1 + 2K_2 < 0$, or $K_1 > 0$; $K_1 + K_2 < 0$).

Upon application of an external field $\vec{H}$, the free energy E in equation (1) gains an additional term, such that $E_{tot} = E - \mu_0 \vec{H} \cdot \vec{M}$. First, we consider the experimental geometry where the field is varied from pointing along the c axis to within the *ab* plane, with the sample aligned so that ϕ remains constant during this measurement. Denoting the angle between the applied field and c axis as γ, the torque that must be applied to hold the sample in place is

$$\tau = \frac{\partial E_{tot}}{\partial \gamma} = -\mu_0 M_s H \sin(\theta - \gamma). \qquad (4)$$

In general the magnetization will rotate to minimize the free energy, $\partial E_{\rm tot}/\partial\theta = 0$, which allows the torque to be expressed equivalently as $\tau = \partial E/\partial\theta$. If the magnetization angle θ were known, measuring the torque would therefore be sufficient to extract the anisotropy constants directly by fitting to the derivative of equation (1).

However, for strongly anisotropic materials like RCo_5 the external field is generally not strong enough to align the magnetization along the direction of the field, so θ remains unknown. To extract anisotropy constants it is therefore necessary to adopt an indirect approach [8]. This method uses the fact that the torque crosses zero when the angles of the applied field and magnetization coincide with the easy angle α. Introducing $\theta' = \theta - \alpha$ and $\gamma' = \gamma - \alpha$, for fields applied at angles close to this zero crossing we have $\tau \approx -\mu_0 M_{\rm s} H(\theta' - \gamma')$. If the leading order term in the torque is linear in θ', i.e. $\tau \approx \theta'/\beta$, then $\tau[1/M_{\rm s} + \mu_0 H\beta] = \gamma'\mu_0 H$, or

$$\eta \equiv \frac{\mu_0 H}{\frac{{\rm d}\tau}{{\rm d}\gamma}} = \mu_0 H\beta + \frac{1}{M_{\rm s}}. \tag{5}$$

${\rm d}\tau/{\rm d}\gamma$ is the (linear) variation of the torque with field angle as τ crosses zero.

Plotting η as a function of applied field should yield a straight line, with the intercept giving the reciprocal of the magnetization $M_{\rm s}$. To obtain an expression for the gradient β in terms of the anisotropy constants, we set $\partial E_{\rm tot}/\partial\theta = 0$, substitute in θ' and perform small angle expansions. This procedure yields

$$\beta = \frac{1}{2K_2 \sin^2 2\alpha + 2\,\cos\,2\alpha(K_1 + 2K_2 \sin^2\alpha)}. \tag{6}$$

Inserting this into equation (5) we have for the specific cases

$$\eta = -\frac{\mu_0 H}{2(K_1 + 2K_2)} + \frac{1}{M_{\rm s}}\ \text{(plane)}, \tag{7}$$

$$\eta = \frac{\mu_0 H}{2K_1} + \frac{1}{M_{\rm s}}\ \text{(axis)}, \tag{8}$$

$$\eta = \frac{\mu_0 H}{2K_2 \sin^2 2\alpha} + \frac{1}{M_{\rm s}}\ \text{(cone)}. \tag{9}$$

For anisotropy in the basal plane a similar procedure may be applied for the azimuthal torque $\tau_\phi = \partial E_{\rm tot}/\partial\gamma_\phi$. Here the field and magnetization are confined to the $\gamma = \theta = 90^\circ$ plane, and γ_ϕ is the azimuthal angle of the applied field. Then,

$$\eta_\phi \equiv \frac{\mu_0 H}{\frac{{\rm d}\tau_\phi}{{\rm d}\gamma_\phi}} = \frac{\mu_0 H}{36|K_4|} + \frac{1}{M_{\rm s}}. \tag{10}$$

2.3. Calculations of torque curves

Equation (4) demonstrates that, if the magnetization magnitude and angle can be calculated for a given applied field, the torque follows immediately. A recently developed framework [31] allows these quantities to be calculated entirely from first principles. The framework partitions $NdCo_5$ into two subsystems, namely itinerant electrons mainly associated with Co and highly-localized Nd-4f electrons. The temperature-dependent free energy of the itinerant electrons is calculated within DFT within the disordered local moment picture [21, 31, 34, 35]. Meanwhile the free energy of the Nd-4f electrons is calculated by statistical mechanics from the eigenvalues of an atomic-like Hamiltonian $\mathcal{H}$. Crucially, $\mathcal{H}$ contains the crystal field, where the coefficients are also calculated from first principles, and also the exchange field originating from the itinerant electrons. The equilibrium magnetization is found by minimizing the total free energy for a given external field and temperature. A complete description of the framework is published elsewhere [31].

3. Results and discussion

3.1. Manifestation of the spin reorientation transition in magnetization measurements

Figure 1 shows the magnetic field dependence of magnetization at $T = 5$, 200, and 300 K for $H \perp c$ and $H \parallel c$. These data were recorded while reducing the field from the maximum value to zero. At 5 K the $M(H)$ curve for $H \perp c$ saturates above $\sim$ 1 T and remains nearly field independent thereafter with a saturation magnetization $M_{\rm s} \approx 10.3(1)\mu_{\rm B}$/f.u. On the other hand, the $M(H)$ data for $H \parallel c$ increase linearly with field at low fields and then curve over, reaching a magnetization of just $\approx 4.1(1)\mu_{\rm B}$/f.u. at 5 T. There is no sign of the upturn in $M(H)$ at higher fields for $H \parallel c$ reported for pulsed field measurements [36]. The $M(H)$ curves in figures 1(a) and (b) clearly demonstrate the occurrence of an SRT in $NdCo_5$ with the easy axis switching from the basal plane to the c axis with increasing temperature between 200 and 300 K. At low field (0.1 T) the anisotropy in M for the two field directions remains significant; $\left(M_{H\perp c}/M_{H\parallel c}\right)$ is $\sim$ 2.5 at 200 K and $\sim$ 0.35 at 300 K, but the sample becomes easier to magnetize along the hard axis at higher fields and the apparent anisotropy is much reduced.

Figure 2(a) shows the dc magnetization versus temperature ($M(T)$) curves in a magnetic field $\mu_0 H = 0.5$ T applied parallel ($H \parallel c$) and perpendicular ($H \perp c$) to the crystallographic c axis of the $NdCo_5$ crystal. These data were recorded in the field-cooled-warming mode, i.e., the crystal was cooled to 5 K in the presence of field and the data were then recorded while warming in the same field. The $M(T)$ curves are almost temperature independent in both field directions for $T < 180$ K. The $M(T)$ values for $H \parallel c$ are lower as the c axis is the hard axis in this temperature range. As the temperature rises above 180 K, $M(T)$ for $H \parallel c$ increases. $|{\rm d}M(T)/{\rm d}T|$ reaches a maximum value (≈ 0.18) at 254 K and $M(T)$ peaks at around 288 K before slowly decreasing thereafter. For the field in the basal plane, ($H \perp c$), $M(T)$ shows a weaker temperature-dependence until about $T \sim 248$ K and it then begins to fall rapidly with temperature. Here, the maximum in $|{\rm d}M(T)/{\rm d}T| \approx 0.16$ occurs at around 289 K. This crossover in $M(T)$ reflects the spin reorientation transition.

The SRT can also be observed using ac susceptibility measurements. The in-phase component of the ac magnetic susceptibility ($\chi'(T)$) was recorded in a dc magnetic field ($\mu_0 H = 0.1$ T) for $H \parallel c$ as shown in figure 2(b) (data normalized with respect to the peak value around 288 K). It is generally expected that a transition which involves the rotation of magnetization between different crystallographic

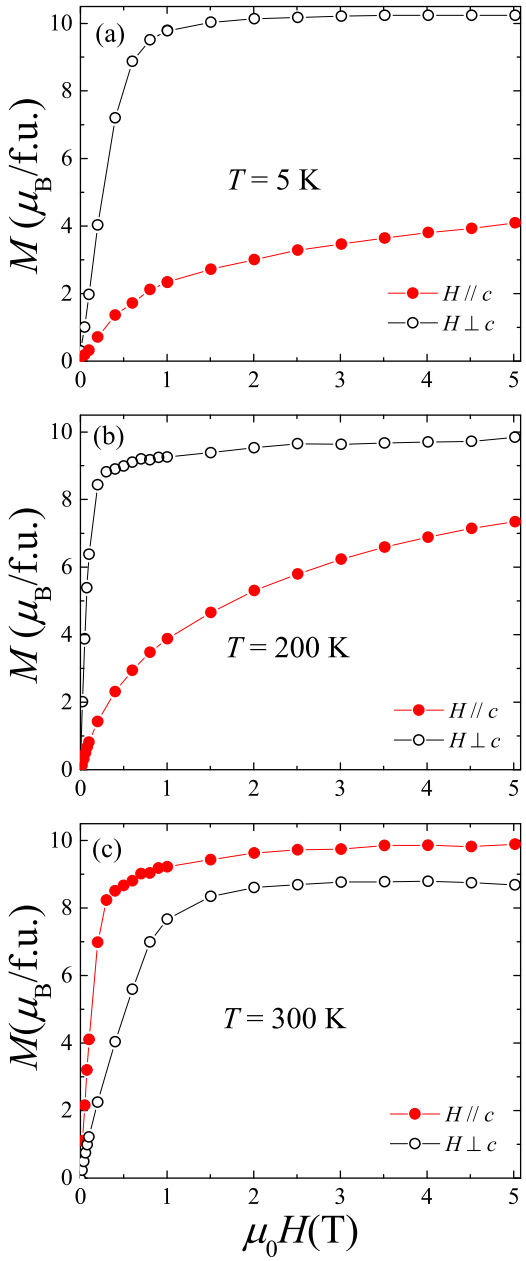

Figure 1. DC magnetization versus field for $H \parallel c$ and $H \perp c$ at (a) $T = 5$ K, (b) 200 K, and (c) 300 K.

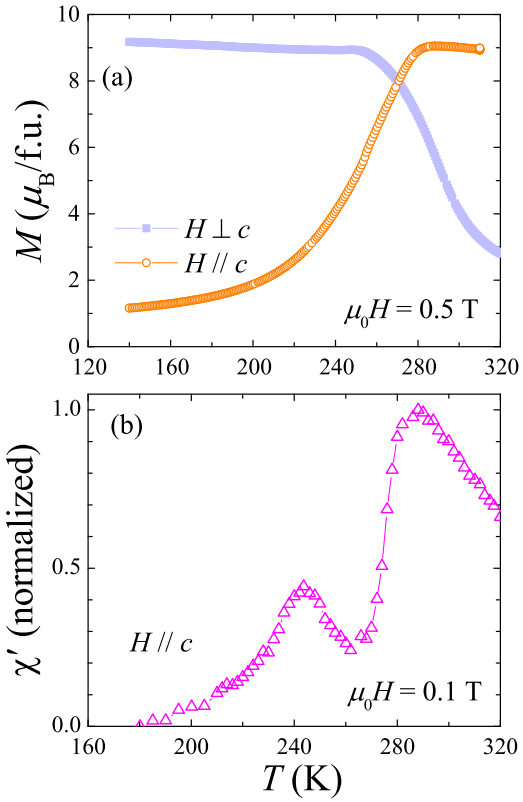

Figure 2. (a) DC magnetization vs temperature for $H \parallel c$ and $H \perp c$ in a magnetic field of $\mu_0 H = 0.5$ T in the region of spin reorientation transition for $NdCo_5$. (b) Temperature variation of ac magnetic susceptibility $\chi'(T)$ ($h_{ac} = 0.3$ mT, $f = 10$ Hz) in a dc magnetic field $\mu_0 H = 0.1$ T.

axes will be accompanied by a modulation in the dynamic susceptibility ($\chi'(T)$) resulting in a peak or a change in the gradient of $\chi'(T)$ (see [37, 38] and references therein). The $\chi'(T)$ curve in figure 2(b) exhibits two well-resolved peaks, centred around 243 and 288 K. The peak at lower temperature occurs as the moments begin to move out of the *ab* plane to form a cone, while the peak at 288 K occurs around the temperature at which the cone closes and the system favours an easy *c* axis, echoing the changes in gradient seen in the dc magnetisation versus temperature data.

3.2. Observation of spin reorientation transition in torque measurements

The spin reorientation transition in $NdCo_5$ was studied using torque magnetometry. Figure 3 shows the change in the torque, τ, at 300 (a) and 200 K (b) as the direction of an applied magnetic field ($\mu_0 H = 0.5$ T) is varied in the *ac* plane. Here, γ is the angle between the applied magnetic field and the *c* axis. The $\tau(\gamma)$ curves are periodic with zero-crossings at 90° intervals, i.e. $\gamma = 0°, 90°, 270°$, etc. At $T = 300$ K, above the SRT, the torque switches very rapidly at $\gamma = 90°$ and 270°, i.e. when the field crosses the *ab* plane. Below the SRT, at $T = 200$ K, the faster switching of torque instead happens at $\gamma = 0°$ and 180°, when the field crosses the *bc* plane. It is noteworthy that the $\tau(\gamma)$ curves at these two temperatures exhibit opposite polarities for a given γ value. For $T = 200$ K, $\tau(\gamma)$ crosses from negative to positive values at 90 (and 270) degrees (see figure 3) indicating an easy plane behaviour. At 300 K, this zero-crossing from negative to positive values of $\tau(\gamma)$ occurs at 180 (and 360) degrees indicating that *c* is the easy axis. Figure 3 also shows the torques calculated from the first principles for $NdCo_5$ as the open triangles.

Considering the $T = 300$ K data first (figure 3(a)) we see that there is rather good agreement between the calculations and measurements. In particular, the calculated torque curves have the same periodicity as the experimental measurements and the same qualitative shape. It is important to note that the calculations are based on a global minimization of E_{tot}, i.e. the magnetization always adopts the lowest energy orientation, regardless of any energy barriers. Performing the minimization in this way allows for the rapid switching of the torque e.g. at $\gamma = 90°$.

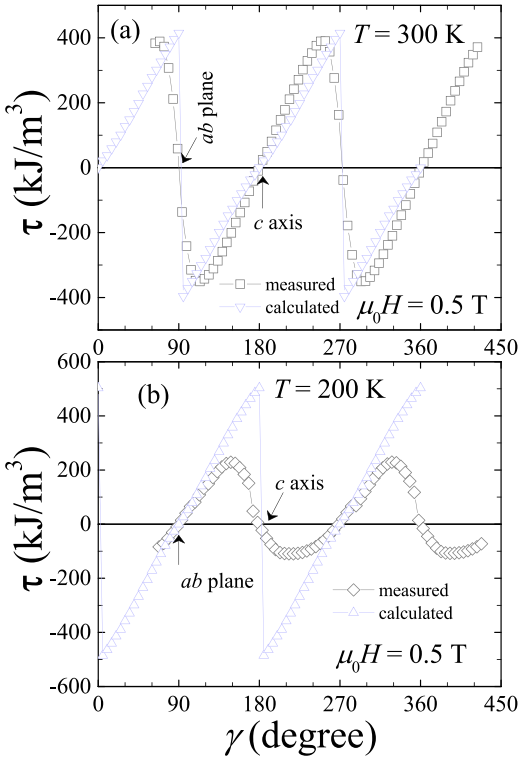

Figure 3. Angular variation of the torque ($\tau(\gamma)$) measured as well as calculated at $\mu_0 H = 0.5$ T at (a) $T = 300$ K and (b) $T = 200$ K.

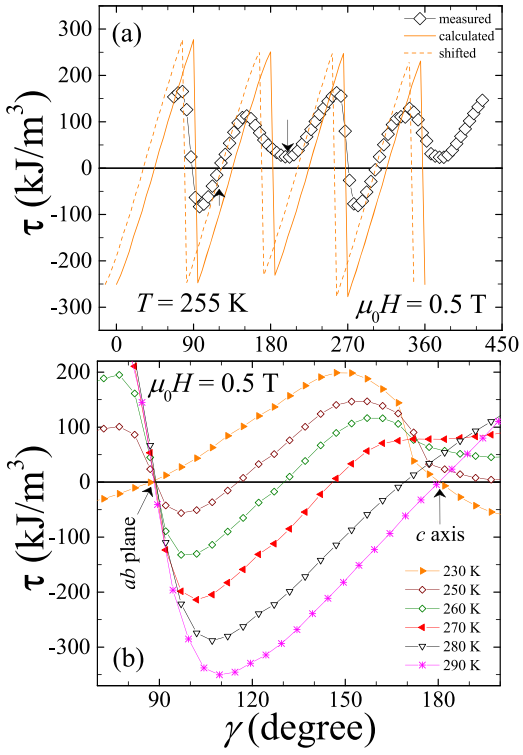

Figure 4. (a) $\tau(\gamma)$ curves measured and calculated at $\mu_0 H = 0.5$ T for $T = 255$ K. (b) Portions of $\tau(\gamma)$ curves (measured) highlighting the position of the negative to positive τ crossing in each curves.

The fact that the measured torque also shows this rapid variation indicates that the experimental conditions also allow for an effectively discontinuous magnetization switch. A possible mechanism for this switch would be the nucleation of a reverse domain along the preferential orientation, which quickly grows to saturation. The magnetization reverses when the projection of the field onto the c axis changes sign. We note that experimentally, the magnetization reversal does not occur instantaneously at $\gamma = 90$, 270° as in the calculations, but rather extends over a region of ±20°. Away from this region the calculations, which describe purely the rotation of a single domain, give a good account of the measured data.

For the data below the SRT at $T = 200$ K (figure 3(b)), we see that the agreement between the calculated and measured torques is less good. The peak torque, calculated to be 503 kJm^{-3}, is measured to be only 226 kJm^{-3}. Indeed, the rapid reversal of magnetization in the calculations occurring at $\gamma = 180°$ is strongly smeared out in the experimental data. This behaviour indicates that the magnetization reversal, which at 300 K was assumed to occur through the rapid growth of a single domain, instead takes place more gradually at 200 K when the easy direction lies in the basal plane.

It is very reasonable to expect that the magnetization reversal mechanism at $\gamma = 180°$ at 200 K is different to that at $\gamma = 90°$ at 300 K. Considering equation (1), the reason for the rapid switch at 300 K is that the anisotropy contribution is identical for magnetization angles of θ and $180° - \theta$, but the latter has a lower interaction energy with the external field as soon as γ increases past $\gamma = 90°$. Reaching this lower energy solution by rotation requires increasing θ, with an associated penalty in the anisotropy energy. At 200 K the analogous situation occurs for magnetization angles of θ and $-\theta$ as γ increases past $\gamma = 180°$; however, the $\theta \to -\theta$ transition can be equivalently described as maintaining a constant θ but increasing the polar angle ϕ by 180°. The anisotropy energy associated with ϕ is determined by K_4 which is expected to be small at these temperatures (see figure 9(b) below). Therefore, the energy barrier of the $\theta \to -\theta$ transition at 200 K will be much smaller than for the $\theta \to 180° - \theta$ transition at 300 K.

We now consider $\tau(\gamma)$ within the SRT. Figure 4(a) shows τ vs γ data recorded within the SRT region at $T = 255$ K with an applied field $\mu_0 H = 0.5$ T in the ac plane. Here, the shape of the $\tau(\gamma)$ curve is different than above and below the SRT. $\tau(\gamma)$ crosses over from positive to negative at $\gamma = 90°$ which corresponds to the ab plane. This is followed by another zero-crossing occurring at $\gamma \approx 120°$ (see arrow pointing upwards) above which the $\tau(\gamma)$ behaves unusually across the interval $120° < \gamma < 270°$. In this region, $\tau(\gamma)$ shows a tendency to crossover from positive to negative values, however, it does not reach zero but rather a minimum at $\gamma \approx 200°$ (see down arrow) before showing an uprise.

The calculations also bear some resemblance with the experiments in the SRT regime. For example, the calculated curve shows an apparent cone anisotropy. Due to the intrinsic approximations of the theory, the calculated zero crossing positions do not show perfect numerical agreement with the experimentally observed ones, for instance deviating by 13° (see solid line) at 255 K. However, correcting for this small numerical deviation (dashed curve) we note that the measured

and calculated data show similar slopes at the zero-crossings. Some differences between the theory and experiments can also be noticed as the measurements show a dip around $\gamma = 200^\circ$ where the calculated data changes the sign. The fact that the measured torque curves do not cross zero at $\gamma = 0$ and 180° implies that the magnetization reversal is incomplete and there is more than one domain.

The above observations nicely illustrate some of the difficulties in understanding torque curves, especially in the presence of domain structures. In order to have the clearest interpretation of torque measurements it is instead desirable to remove the domain structure by working with a large field, and keeping the applied field close to the easy direction of magnetization. It is this approach we follow in order to extract anisotropy constants below.

Figure 4(b) shows portions of the $\tau(\gamma)$ curves at various temperatures belonging to the SRT regime, as indicated. At temperatures well above and below the SRT the $\tau(\gamma)$ curves are similar to those shown in figure 3. The value of γ where $\tau(\gamma) = 0$ shifts systematically with temperature. We use the difference ($\Delta\gamma$) between this angle and position of the zero-crossing at the c axis to determine the easy direction versus temperature (see figure 5). The feature around 250 K suggests that at this field the SRT may proceed in two steps. Some other studies report a rapid change in α at both ends of the SRT [8, 26, 39], while others suggest a more rounded transition [12]. In zero field, it is reported that the SRT in $NdCo_5$ occurs over a temperature interval, ΔT_{SRT}, of approximately 40 K [e.g. ($242 < T < 283$ K) [26] or ($248 < T < 286$ K) [39]]. It is also reported that the width of the SRT broadens in magnetic field [17] where for $H \parallel c$ the SRT begins at ~ 285 K but is complete only at temperatures well below 245 K, while for $H \perp c$ the spin reorientation begins at ~ 245 K but ends at temperature well in excess of 285 K [12, 17, 39]. In the present study the magnetization versus temperature data (see e.g. figure 2(a)) captures the broadening of the transition, while in our torque data, the SRT appears much sharper ($\Delta T_{SRT} = 45$ K), even though the measurements are performed in 0.5 T, because we fix the field and rotate the sample.

Figure 6 shows the variation of magnetization angles of the Nd and Co sublattices (calculated) with the direction of applied magnetic field. If the magnetization always pointed in exactly the same direction as the field, the curves would lie on the dotted lines. If the Nd and Co always pointed in exactly the same direction as the field, the two curves (orange and blue) would lie on top of each other. The fact that they are distinct shows that there is canting between the two sublattices like in $GdCo_5$ [21]. The canting is about 10° at 255 K. It is also worthwhile to note that the Nd (blue line) prefers to stay closer to 90° or 270°, while the Co (orange line) prefers to stay closer to 0° or 180°. This is the reason why the Co sublattice lags for $0 \leqslant \gamma \leqslant 90^\circ$ and leads for $90^\circ \leqslant \gamma \leqslant 180^\circ$. The rapid jumps in magnetization angle coincide with the jumps in the torque; this is the magnetization jumping to a new minimum. Usually, there would be energy barriers associated with this. To sum up, the general problem with torque measurements on strongly anisotropic materials is clearly apparent from the big difference seen here between the applied magnetic field angle and

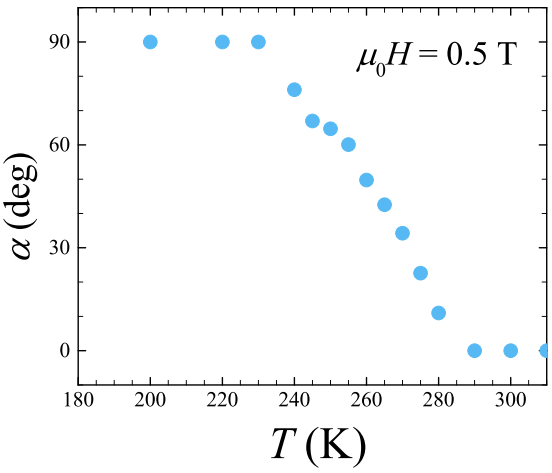

Figure 5. Temperature dependence of the α (angle between easy axis and c axis) at $\mu_0 H = 0.5$ T for $NdCo_5$. The temperature interval spanned by the SRT is identified at this field value. The easy axis is in the ab plane below $T = 220$ K, in a cone for $220 < T < 320$ K and is along c above $T = 320$ K.

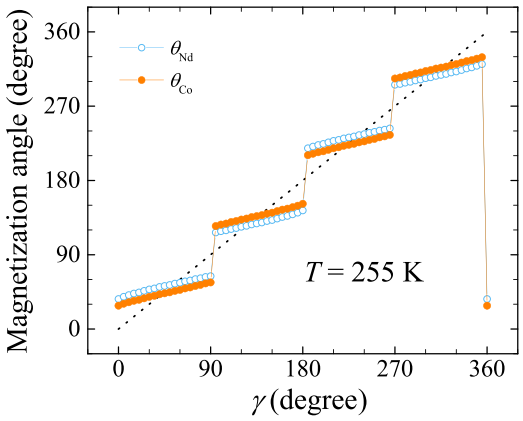

Figure 6. Angles of Nd and Co magnetization as a function of applied field angle.

the magnetization angle (except close to the easy direction). The occurrence of canting between the Nd and Co sublattice also justifies the K_i being the effective values. The system behaves as expected, i.e., Nd exhibits a planar anisotropy while Co has a uniaxial anisotropy.

3.3. Estimation of magnetocrystalline anisotropy constants for $NdCo_5$

3.3.1. Angular variation of torque in the plane containing the c axis. We are now in a position to estimate the magnetocrystalline anisotropy constants (K_1 and K_2) in the region spanned by SRT using the torque data. Equation (9) implies that a plot of $H(\frac{d\gamma}{d\tau})$ $(= \eta)$ vs H should yield a line, the slope and intercept of which give K_2 and M_s, respectively. In order to estimate these, τ vs γ data were recorded in close proximity to the easy axis. A curve at 260 K that is typical of the data collected is shown in figure 7(a). These data were recorded for only a few degrees above and below the zero crossing in $\tau(\gamma)$, where the approximations used to derive equation (5) are valid. For each

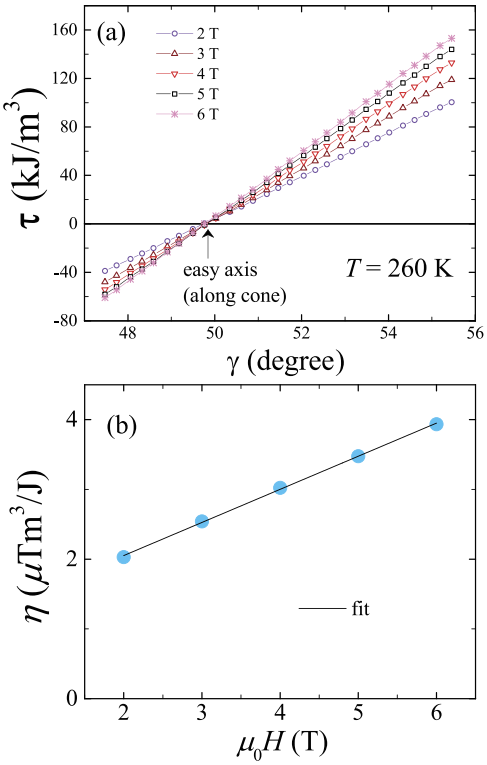

Figure 7. $\tau(\gamma)$ curves for $2 \leqslant \mu_0 H \leqslant 6$ T at $T = 260$ K obtained for γ close to the easy direction (along cone) for $NdCo_5$. (b) η vs H at $T = 260$ K displaying a linear behaviour.

of these curves, the measuring field was applied at a value of γ lying a few degrees below the zero-crossing and the data were then recorded while increasing γ in small steps. All the curves shown in figure 7(a) are linear in γ over the chosen $\Delta\gamma$ interval. The gradients of these curves were extracted to obtain η vs H as shown in figure 7(b) which is found to be linear. Using equation (9), K_2 is found to be 1.18(1) MJ m^{-3} which in turn gives $K_1 = -1.58(1)$ MJ m^{-3} from equation (3) ($\alpha = 55°$ at 260 K from figure 5). Using this method, the K_1 and K_2 values were obtained at 5 K increments in the SRT region ($240 < T < 285$ K).

In addition, using torque data and equation (7) gives $K_1 + 2K_2$ below the SRT region while at temperatures above the SRT, equation (8) can be used to give K_1. Accordingly, the temperature variation of K_1 ($K_1 + 2K_2$) above (below) the SRT have also been obtained (see supplementary file for details stacks.iop.org/JPhysCM/32/255802/mmedia).

3.3.2. Angular variation of the torque in the basal plane. The anisotropy constant K_4 can be obtained from the angular variation of τ in the *ab* plane using equation (10). $\tau_\phi(\gamma_\phi)$ data were recorded at several magnetic fields ($2 \leqslant \mu_0 H \leqslant 6$ T). $\tau_\phi(\gamma_\phi)$ at $T = 200$ K that is typical of the data collected is shown in figure 8. Following a similar protocol to that discussed above, η vs H is determined as shown in the inset panel of figure 8. Equation (10) gives $K_4 = 0.152$ MJ m^{-3}. Similar measurements were carried out at other temperatures ($5 < T < 300$ K) to give the temperature dependence of K_4 and M_s.

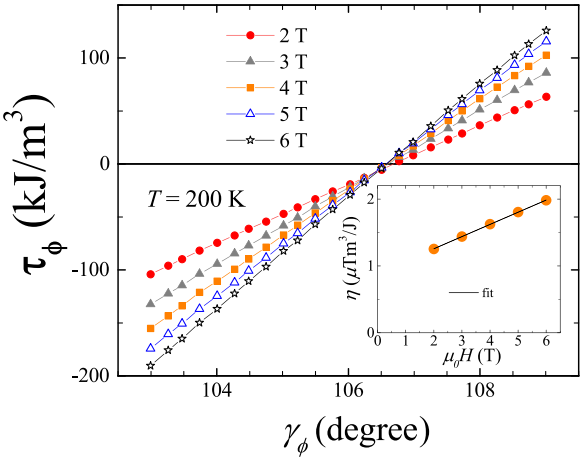

Figure 8. High field $\tau_\phi(\gamma_\phi)$ curves at 200 K obtained in the vicinity of easy axis within the *ab* plane of single-crystal $NdCo_5$. Inset shows η against H.

3.4. Temperature dependence of the magnetocrystalline anisotropy constants

The temperature dependence of K_1 and K_2 across the regime of the SRT is displayed in figure 9. We have also shown a few data points for $K_1 + 2K_2$ (determined using equation (7)) below and K_1 (determined using equation (8)) above the SRT (see supplementary file for data over the full temperature range studied). As expected, the K_1 values (closed stars) are negative in the easy cone region (SRT). Their magnitude decreases monotonically with increasing temperature and K_1 changes sign at the completion of SRT. In the easy *c* axis region, K_1 is positive and increases with temperature. Our K_1 values agree well with those obtained for $NdCo_5$ single crystal by Ohkoshi *et al* [17] (shown by open stars in figure 9(a)). However, our K_1 values are not in agreement with the studies reported for $NdCo_5$ thin films [28] or for the aligned powder [12] (see supplementary file).

K_2 is positive in the SRT region and falls slightly with increasing temperature until about $T = 275$ K where there is an increase in K_2. $K_1 + 2K_2$ is negative below the SRT as expected for an easy basal plane. In the SRT region, the $K_1 + 2K_2$ values are positive and weakly-dependent on the temperature except at the high-temperature end of SRT where there is an upturn in the value of $K_1 + 2K_2$. The apparent divergence in K_2 at $T \approx 280$ K illustrates the failure of equation (9) at the completion of the transition. Equation (9) is valid in the regime that τ is proportional to θ (section 2.2) but this component disappears as $\alpha \to 0$. Indeed, equation (9) diverges in this limit. The $K_2(T)$ dependence is in reasonable agreement with [17] (open triangles in figure 9(a)). However, our values of K_2 are higher than those reported in other studies [8, 12, 28].

Figure 9(b) shows the temperature dependence of K_4 in the temperature interval $5 < T < 280$ K. The values of K_4 are found to be positive and are much smaller than K_1 and K_2 over the entire temperature range. K_4 falls monotonically with increasing temperature and approaches zero at $T \sim 280$ K, the temperature around which the SRT is complete. Our $K_4(T)$ data agree with those of Klein *et al* [8] (open squares in figure 9(b)) who report data over a narrower temperature

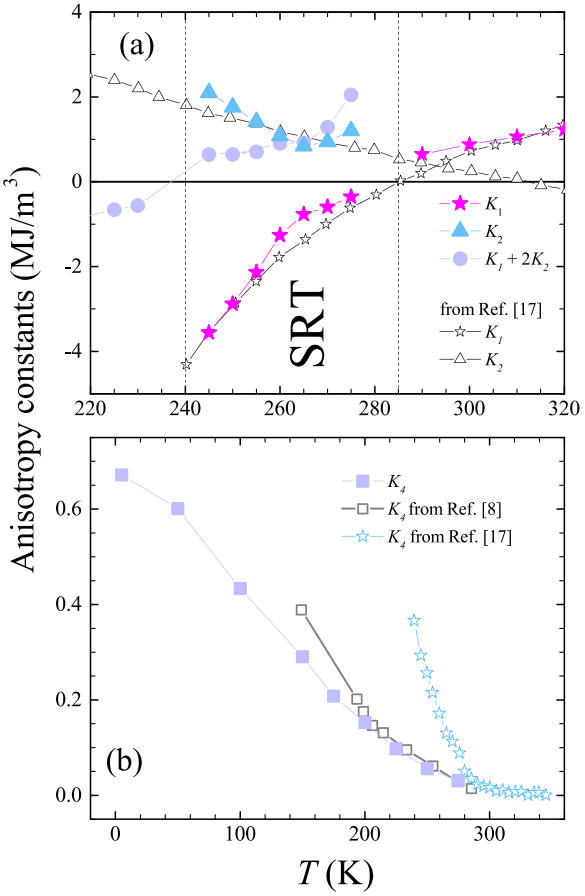

Figure 9. (a) K_1, K_2 and $K_1 + 2K_2$ plotted against T for $NdCo_5$. (b) Temperature variation of the anisotropy constants K_4. For comparison, the data from some previous studies are also shown.

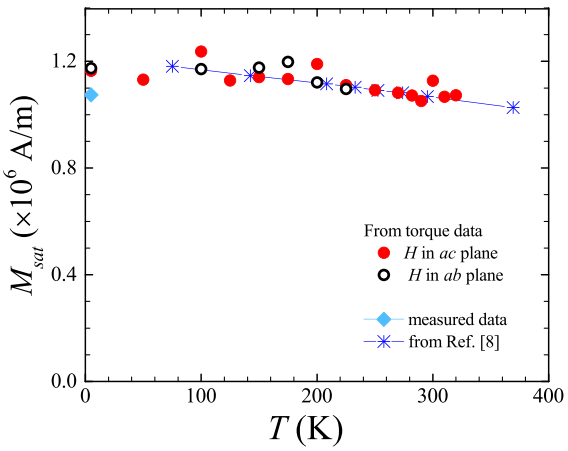

Figure 10. M_s vs T for $NdCo_5$ estimated from the torque magnetometry data. M_s from the direct measurements is shown for $T = 5$ K. $M_s(T)$ from [8] is also shown for comparison.

range. However, they deviate significantly from the only other data available in the literature [17] (stars in figure 9). A possible reason for this deviation is that equation (10) assumes that the magnetization is confined to the basal plane, which is not satisfied during the SRT. On the other hand, the method should be robust at lower temperatures.

The validity of the present results can be checked by examining the values of M_s and its temperature dependence (see figure 10) obtained from the torque measurements carried out with the field in either *ac* or the *ab* plane. The M_s values from our torque data agree very well with those reported by Klein *et al* [8], as well as the M_s values obtained by directly measuring the magnetization using dc magnetization.

4. Summary and conclusions

We have performed a detailed experimental and theoretical study of the spin reorientation transition and the magnetocrystalline anisotropy in the R–TM based permanent magnet $NdCo_5$ using torque magnetometry complemented with magnetic susceptibility measurements. Single crystals of $NdCo_5$ were prepared by the optical FZT technique. Magnetization measurements, both ac and dc, show a clear evidence of the SRT. Using the torque magnetometry, we have studied the magnetic behaviour of the $NdCo_5$ crystal at temperatures around the SRT. The occurrence of this transition in $NdCo_5$ is indicated by a reversal in the polarity of torque curves ($\tau(\gamma)$) as the temperature changes. In the region of the SRT, the torque curves exhibit unusual features different to those seen below and above the transition. The change in easy axis with temperature is apparently seen in the torque data recorded in the SRT region. To understand the experimental results, we have carried out first-principles calculations based on density-functional theory and the disordered local moment picture of finite temperature magnetism to calculate the torque curves. Our calculations also allowed us to resolve the Nd and Co magnetizations and thus leads to a clear understanding of the physics of the SRT. The magnetization angles of Nd and Co are found to be distinct indicative of a canting between the two sublattices. Using the high field torque measurements ($2 \leqslant \mu_0 H \leqslant 6$ T) carried out in the close vicinity of the easy axis, we estimate the anisotropy constants (K_1, K_2 and K_4) and their temperature dependence across the SRT.

In terms of future work, the main discrepancy between the calculated torque curves and experiment is the nature of magnetization reversal, which is determined by the nucleation and propagation of reverse domains. Being able to accurately model such effects is a significant challenge, but would allow an even clearer understanding of the torque curves, and also of the ac susceptibility and initial dc magnetization data.

Acknowledgments

This work is a part of PRETAMAG project funded by the Engineering and Physical Sciences Research Council, Grant No. EP/M028941/1 and EP/M028771/1. M Ciomaga Hatnean is acknowledged for assistance with single crystal growth. We thank P A Goddard, E Mendive-Tapia, G Marchant, A Tedstone, K Götze and M J Pearce for useful discussions.

ORCID iDs

Santosh Kumar https://orcid.org/0000-0002-3174-3144
Christopher E Patrick https://orcid.org/0000-0002-1843-1269

Rachel S Edwards https://orcid.org/0000-0003-2550-3627
Geetha Balakrishnan https://orcid.org/0000-0002-5890-1149
Martin R Lees https://orcid.org/0000-0002-2270-2295
Julie B Staunton https://orcid.org/0000-0002-3578-8753

References

[1] Buschow K J H and Brouha M 1976 *J. Appl. Phys.* **47** 1653
[2] Buschow K H J and Den Broeder F J A 1973 *J. Less-Common Met.* **33** 191
[3] Hoffer G and Strnat K 1966 *IEEE Trans. Magn.* **2** 487
[4] Strnat K, Hoffer G, Olson J, Ostertag W and Becker J J 1967 *J. Appl. Phys.* **38** 1001
[5] Tatsumoto E, Okamoto T, Fujii H and Inoue C 1971 *J. Phys. Colloq.* **32** 550
[6] Alameda J M, Deportes J, Givord D, Lemaire R and Lu Q 1980 *J. Magn. Magn. Mater.* **15** 1257
[7] Alameda J M, Givord D, Lemaire R and Lu Q 1981 *J. Appl. Phys.* **52** 2079
[8] Klein H P, Menth A and Perkins R S 1975 *Physica* B **80** 153
[9] Daalderop G H O, Kelly P J and Schuurmans M F H 1991 *Phys. Rev.* B **44** 12054
[10] Daalderop G H O, Kelly P J and Schuurmans M F H 1996 *Phys. Rev.* B **53** 14415
[11] Steinbeck L, Richter M and Eschrig H 2001 *Phys. Rev.* B **63** 184431
[12] Bartholin H, Van Laar B, Lemaire R and Schweizer J 1966 *J. Phys. Chem. Solids* **27** 1287
[13] Ermolenko A 1976 *IEEE Trans. Magn.* **12** 992–6
[14] Ermolenko A 1979 *IEEE Trans. Magn.* **15** 1765–70
[15] Radwanski R J, Franse J J M, Quang P H and Kayzel F E 1992 *J. Magn. Magn. Mater.* **104** 1321
[16] Ibarra M R, Morellon L, Algarabel P A and Moze O 1991 *Phys. Rev.* B **44** 9368
[17] Ohkoshi M, Kobayshi H, Katayama T, Hirano M, Katayama T and Tsushima T 1976 *AIP Conf. Proc.* **29** 616
[18] Pareti L, Moze O, Solzi M and Bolzoni F 1988 *J. Appl. Phys.* **63** 172
[19] Nordstrom L, Brooks M S S and Johansson B 1992 *J. Phys.: Condens. Matter.* **4** 3261–72
[20] Bartashevich M, Goto T, Radwanski R and Korolyov A 1994 *J. Magn. Magn. Mater.* **131** 61
[21] Patrick C E, Kumar S, Balakrishnan G, Edwards R S, Lees M R, Petit L and Staunton J B 2018 *Phys. Rev. Lett.* **120** 097202
[22] Wernick J H and Geller S 1959 *Acta Crystallogr.* **12** 662
[23] Steinbeck L, Richter M and Eschrig H 2001 *J. Magn. Magn. Mater.* **226** 1011
[24] Pourarian F, Satyanarayana M V and Wallace W E 1981 *J. Magn. Magn. Mater.* **25** 113
[25] Patterson C, Givord D, Voiron J and Palmer S B 1986 *J. Magn. Magn. Mater.* **54** 891
[26] Sousa J B, Moreira J M, Del Moral A, Algarabel P and Ibarra R 1990 *J. Phys.: Condens. Matter.* **2** 3897
[27] Nikitin S A, Skokov K P, Koshkid'ko Y S, Pastushenkov Y G and Ivanova T I 2010 *Phys. Rev. Lett.* **105** 137205
[28] Seifert M, Schultz L, Schafer R, Neu V, Hankemeier S, Rossler S, R Frömter and Oepen H P 2013 *New J. Phys.* **15** 013019
[29] Patrick C E and Staunton J B 2019 *J. Phys.: Condens. Matter.* **31** 305901
[30] Sucksmith W and Thompson J E 1954 *Proc. R. Soc.* A **225** 362
[31] Patrick C E and Staunton J B 2019 *Phys. Rev. Mater.* **3** 101401(R)
[32] Singh R P, Smidman M, Lees M R, McK Paul D and Balakrishnan G 2012 *J. Cryst. Growth* **361** 129
[33] Miller J F and Austin A E 1973 *J. Cryst. Growth* **18** 7
[34] Mermin N D 1965 *Phys. Rev.* **137** A1441
[35] Gyorffy B L, Pindor A J, Staunton J, Stocks G M and Winter H 1985 *J. Phys. F: Met. Phys.* **15** 1337
[36] Zhang F Y, Gignoux D, Schmitt D, Franse J J M and Kayzel F E 1994 *J. Magn. Magn. Mater.* **136** 245
[37] Balanda M 2013 *Acta Phys. Pol.* A **124** 964
[38] Topping C V and Blundell S J 2019 *J. Phys.: Condens. Matter.* **31** 013001
[39] Algarabel P A, del Moral A, Ibarra M R, Sousa J B, Moreira J M and Montenegro J F 1987 *J. Magn. Magn. Mater.* **68** 177